Astrophysics and Space Science (2022) 367:59
https://doi.org/10.1007/s10509-022-04090-1

ORIGINAL ARTICLE

Geomagnetic secular variation consequences on the trajectories of radiation belt trapped particles

Alvaro R. Gutierrez Falcón[1] · Bruno S. Zossi[2,3] · Hagay Amit[4] · Ana G. Elias[1,2,3]

Received: 8 March 2022 / Accepted: 25 May 2022

Abstract
The trajectories of energetic particles trapped by the geomagnetic field, as those composing the Earth's Van Allen radiation belts, are usually defined by three cyclic motions: gyration, bounce along field lines and drift around the Earth, which are all controlled by this field. The geomagnetic dipole, in turn, has been declining at a rate of ∼5% every hundred years since at least ∼1840. Even with the possibility of a recovery without an extreme event, the global field intensity will very probably continue to decrease in the near future with a consequent weakening of our planet's magnetic shield capacity. The expected variations in trapped particle trajectories are analyzed in the present work through an analytical approach considering the observed axial dipolar geomagnetic field component and its secular variation. The variations expected on the mirror point altitude and on the boundary of Störmer forbidden zone are assessed along the period 1900-2020. The structures here analyzed could approximate plausible radiation belt changes for a continuously weakening geomagnetic dipole which might have numerous consequences for technologies that operate in space.

Keywords Magnetic fields · Trapped particles · Radiation belts · Geomagnetic field · Trapped particle trajectory · Mirror point

1 Introduction

The Earth's magnetosphere varies in timescales from minutes, or less, to thousands of years in response to changes in solar conditions and the geomagnetic field (Siscoe 1976). Regarding long-term timescales over a century, averaging all variability sources, the geomagnetic field secular variation becomes the main forcing of trends that may remain. Over such long timescales, even the Gleissberg cycle which may be present in forcings of solar origin (e.g. Feynman and Ruzmaikin 2014) is expected to be averaged out. The main Earth's magnetic field has been decaying at a rate of ∼5% per century since at least 1840 (Olson and Amit 2006; Finlay 2008; Finlay et al. 2016) or even earlier (Gubbins et al. 2006; Poletti et al. 2018). The intensity of the global field will most likely continue to decrease in the near future (Aubert 2015; Sanchez et al. 2020) with a consequent weakening of our planet's magnetic shield (Heirtzler 2002; Tarduno 2018).

Changes in the geomagnetic field have a major impact on trapped particles in Earth's Van Allen radiation belts. In radiation belt models, trapped particle fluxes are mapped in the (B, L) magnetic coordinate system (McIlwain 1961). The shell parameter L denotes the dipole-like shell where the particle is trapped and corresponds to the equatorial distance to the field line in Earth radii units ($R_E = 6371$ km), while B is the magnetic intensity at which the particle is locally mirroring. Lindstrom and Heckman (1968) were among the first to study the consequences of the Earth's magnetic field changes on trapped particles composing the radiation belts. Their study was mainly focused on comparing the B-L space for $0.20 < B < 0.24$ (in Gauss units) and $1.2 < L < 1.8$ estimated with different geomagnetic field models. When particle losses or redistributions during a drift

✉ A.G. Elias
aelias@herrera.unt.edu.ar

1 Departamento de Física, Facultad de Ciencias Exactas y Tecnología, Universidad Nacional de Tucumán, Av. Independencia 1800, 4000 Tucumán, Argentina

2 Laboratorio de Ionosfera, Atmosfera Neutra y Magnetosfera - LIANM, Facultad de Ciencias Exactas y Tecnología, Universidad Nacional de Tucumán, Av. Independencia 1800, 4000 Tucumán, Argentina

3 INFINOA, CONICET-UNT, 4000 Tucumán, Argentina

4 CNRS, Laboratoire de Planétologie et Géosciences, Nantes Université, Nantes, France

Published online: 09 June 2022

period are negligible, the flux and spectra are the same for all points having the same B and L. Lindstrom and Heckman (1968) analyzed the time variation of B-L trace in altitude for different longitudes. They obtained an altitude decrease from 1965 to 1975 for particles at the same B and L values due to the variation of the non-dipolar components of the field. If the field would have been purely dipolar, with a decreasing dipole moment, the altitude of particles at the same B and L would remain unchanged with time. In fact, they analyzed the South Atlantic Anomaly region, SAA, where the differences between the actual Earth's magnetic field and a dipolar field are strongest (Bloxham et al. 1989; Terra-Nova et al. 2017). This height decrease is then obtained as a result of using a time-dependent field to assess the B-L space.

In a later work, Heckman and Lindstrom (1972) analyzed the secular decrease of the axial dipolar moment of the Earth's magnetic field, M_z, in connection again to B-L space but this time through the theoretical analysis of a particle's motion in an ideal dipolar field considering the adiabatic invariants. They obtained an inward drift of particles accompanied with an increase in energy and particle flux, a decrease of the mirror point height, and the invariance of the pitch angle α (angle between the particle's velocity direction and the magnetic field line) and of the mirror point latitude, λ_m.

Farley et al. (1972) considered the effects of the secular decrease of M_z on the energetic protons of the Van Allen inner radiation belt in two ways: over the diffusion coefficient in the equation of the distribution function, and through the induced electric field that drives these protons radially inward and accelerates them to higher energies. Solving the case of equatorially trapped particles, they obtained an increase in the distribution function at the geomagnetic equator for energetic inner radiation belt protons.

Schulz and Paulikas (1972), in a similar analysis to Heckman and Lindstrom (1972), also demonstrated that the secular decrease of M leads to a contraction of the adiabatic drift shells and to an acceleration, or energization, of the trapped particles. They used the field intensity at the magnetic equator at the Earth's surface instead of M_z, which was 0.31 Gauss at the time, and obtained a 0.05% decrease per year in L that means a drift shell contraction. They also demonstrated that a drift shell secular contraction occurs at constant α and λ_m, and an increase of the kinetic energy.

In a different approach, Pu et al. (2002) designed a drift shell tracing method (DSTM) and obtained results consistent with the previous mentioned works. They showed that the inductive electric field associated with the long-term variation of the magnetic field of the Earth drives the trapped particles inward increasing the fluxes at low L values. The DSTM, in addition to the dipolar term, also takes into account the secular changes of multipole terms which reinforce the deformation of the L-shells and provide additional contributions to the long term variation of the radiation environment, especially in the SAA.

Another approach to predict the variability of some magnetosphere characteristics in terms of the geomagnetic field is through scaling relations in terms of M_z and the dynamic pressure of the solar wind $P_{\rm dyn}$, which lead to first-order approximations of the average geomagnetic field effects. A strong assumption for scaling relations validity is that the system reacts in a self-similar way to changes in the dipole strength. This can only be valid as long as the internal field is dominated by its dipolar part and if the dipole axis remains more or less aligned with the rotation axis, as emphasized by Vogt and Glassmeier (2001).

The magnetopause position, $R_{\rm mp}$, even though not directly linked to radiation belts, is a key magnetosphere parameter which serves as a characteristic measure of its size and an external limit for charged particle populations, such as radiation belts, the ring current and the plasmasphere. It scales with M_z and P_{dyn} according to (Siscoe 1971; Siscoe and Chen 1975; Saito et al. 1978)

$$R_{\rm mp} \propto {M_z}^{1/3} P_{\rm dyn}^{-1/6} \tag{1}$$

This equation can be derived analytically based on the equilibrium condition between the dynamic pressure of the solar wind and the magnetic pressure of the magnetosphere at the subsolar point on the magnetopause, assuming that the thermal solar wind and magnetosphere pressures are negligible, and the magnetic pressure of the solar wind is also negligible with respect to the two pressures considered. Siscoe and Chen (1975) also deduced that the plasmapause position, $R_{\rm pp}$, decreases with M_z slower than $R_{\rm mp}$, thus the fraction of the magnetosphere occupied by the plasmasphere increases with decreasing M_z.

Schulz (1975) analyzed scaling laws for the radial-diffusion coefficients, $D_{\Phi\Phi}$, that affect the Earth's radiation belts, in particular inner radiation belt protons, for a time varying axial dipolar field configuration. Two mechanisms were considered for magnetospheric radial diffusion, both conserving adiabatic invariants. One involves magnetic impulses caused by fluctuations in the solar wind pressure, denoted by the diffusivity ${D_{\Phi\Phi}}^{(m)}$. The other involves electrostatic impulses caused by fluctuations in the rate of energy dissipation at the magnetopause and neutral sheet, denoted by the diffusivity ${D_{\Phi\Phi}}^{(e)}$. Neglecting the solar modulation, that is considering constant average solar conditions, and considering particles' mirror point at the equator, the scaling relationships for a given Φ (the third adiabatic invariant) were derived analytically (Schulz 1975):

$${D_{\Phi\Phi}}^{(m)} \alpha {M_z}^{16/3} \Phi^{-6} \quad \text{and} \quad {D_{\Phi\Phi}}^{(e)} \alpha {M_z}^{17/3}\, \Phi^{-6} \tag{2}$$

Consequently, both diffusivities (${D_{\Phi\Phi}}^{(m)}$ and ${D_{\Phi\Phi}}^{(e)}$) undergo roughly the same modulation with M_z: for a 50% M_z

increase $D_{\Phi\Phi}$ is expected to increase by a factor of ∼10 and for a 50% M_z decrease it is expected to decrease by a factor of ∼40.

Fei et al. (2006) studied the radial diffusion mechanism during magnetic storms. They solved a radial diffusion equation to obtain scaling relations for the diffusion coefficients focusing on short-term variations. Their diffusion coefficients are not in complete agreement with those given in Eq. (2) but, nevertheless, they also increase with increasing M_z and with decreasing Φ.

Vogt and Glassmeier (2000) analyzed a more extreme scenario, considering a quadrupolar geomagnetic field as a feasible high-altitude morphology during a polarity transition to understand possible features of the paleomagnetosphere and of its trapped particle populations. They focused on a field capability of capturing particles based on geometrical criteria for a pure axial quadrupole configuration. They obtained two separate regions of trapped particles, one on each hemisphere, which led to two radiation belts.

Vogt and Glassmeier (2001) highlighted that the validity of these scaling relations depends essentially on whether the magnetopause scaling given by Eq. (1) describes correctly R_{mp} variations, and on the whole system actually behaving self-similarly with respect to changes of the dipole strength. This last condition may be violated for strong southward interplanetary magnetic field, B_z, and high geomagnetic activity levels. However, solar wind average steady behavior on the timescale of interest in secular or paleo studies may guarantee self-similarity. Under a stronger additional assumption, a scaling equation for the ring current extent, R_R, is deduced which can be roughly written as

$$R_R \alpha {M_z}^{1/4} \tag{3}$$

Glassmeier et al. (2004), even though not treating directly trapped energetic particles in the magnetosphere in their derivation of Dst index scaling, explicitly showed that the volume of the magnetospheric region where particle trapping is possible, V_{RC}, scales with M_z as

$$V_{\mathrm{RC}} \alpha {R_{\mathrm{mp}}}^3 \alpha M_z \tag{4}$$

and derived R_{pp} scaling, neglecting solar wind effect variations, as

$$R_{\mathrm{pp}} \alpha {M_z}^{-5/6} \tag{5}$$

which is opposite to the trend suggested by Siscoe and Chen (1975). However, Glassmeier et al. (2004) also noticed that, since R_{mp} and R_{pp} have opposite variation with M_z, for extremely low M_z values the plasmapause position may be larger than the magnetopause distance, which is "unreasonable". Therefore, the scaling derived is only applicable for a certain range of M_z values.

The scaling relation for R_{mp} was also analyzed by Zieger et al. (2006) through MHD simulations of the paleomagnetosphere varying M_z at different values of B_z. They found a power law with scaling exponents different than 1/3 (the theoretically expected one), where the extent of the deviation was found to be controlled by the magnitude of B_z, being greater for strongest values and almost zero when it vanishes.

Vogt et al. (2007) analyzed the variation of differential particle fluxes during periods of reduced dipole moment together with the energy and rigidity cutoff changes through scaling relations. In the case of particle dynamics constrained by adiabatic invariants, as it is the case of radiation belt trapped particles, they studied their ability to reach the upper atmosphere through the open field lines, but they did not consider the possibility of an inward drift of trajectory shells, together with the consequent energization of trapped particles at that shell, due to M decrease.

Stadelmann et al. (2010), in a study of energetic particles in the magnetosphere, presented results of a simulated magnetosphere with a decreasing dipole moment together with the case of an increasing quadrupolar component. They analyzed the trajectories of energetic particles but considered those which finally reach Earth's surface rather than trapped ones. They found that the impact area increases with increasing particle energy or with decreasing magnetic field.

Cnossen et al. (2012) used simulations with the Coupled Magnetosphere-Ionosphere-Thermosphere model. In the case of the magnetopause stand-off distance they found that the theoretical scaling of R_{mp} is too weak (that is, the scaling exponent in Eq. (1) should be greater than 1/3). The reason is a strong increase of the ionospheric conductance with decreasing dipole moment, which leads to a strengthening of the field-aligned currents. These currents generate magnetic fields that are opposite to the main field on the nose of the magnetosphere, while they add to it on the flanks. This results in a stronger compression of the nose of the magnetosphere with diminishing dipole strength larger than expected from the theoretical scaling, while the flanks are less compressed than expected.

Tsareva et al. (2020) studied changes in the shape of the Earth's radiation belts and energy spectra of charged particles in them considering the superposition of axial dipolar and quadrupolar components. A reversal scenario was proposed consisting in a decrease of the dipole component while keeping constant the quadrupole. The structure and dynamics of the radiation belts were determined by the ratio between the sources and losses of charged particles. A gradual reduction of radiation belts was found during the reversal, where the regions of trapped charged particles became asymmetrical with respect to the equatorial plane. Finally, two symmetric trapped regions, one on each hemisphere were obtained for a pure axial quadrupole magnetosphere as in Vogt and Glassmeier (2000).

Bourdarie et al. (2019) studied the slow variation of high-energy ($E > 82$ MeV) proton flux at 800 km height due to the secular drift of the Earth's main magnetic field and to solar cycle variations for the period 1900-2050. They considered IGRF-12 during 1900-2015 and a field prediction for the period 2015-2050 based on data assimilation using the coupled Earth numerical dynamo model of Aubert et al. (2013). This proton flux, mostly concentrated over the SAA region, is assessed from the OPAL (Onera Proton Altitude Low) model. Based on the results of Boscher et al. (2014) which showed that considering changes in the maximum equatorial pitch-angle, MePA, is equivalent to taking into account the effect of the SAA drift over time on the trapped particle distribution at L shells with $L < 2.5$, Bourdarie et al. (2019) introduced MePA predicted variation in the OPAL model. In fact, Boscher et al. (2014) observed a clear, almost linear, pitch angle increase with the SAA drift along the period 1978-2008. Bourdarie et al. (2019) obtained a modulation of the energetic proton flux amplitude clearly linked to the solar activity cycle and a global decrease along the period 1900-2050 linked to the secular drift of the Earth's core magnetic field. Note that, under a larger dipole tilt, with the axial dipolar component still the strongest, the MePA variation is less pronounced, and that for a perfect axial centered dipole with only its dipolar moment intensity change, there is no variation in MePA at all.

An alternative estimation of the geomagnetic field secular variation effect on trapped particles can be done considering the analysis of charged particles trajectories in a dipolar field (Störmer 1955). He showed that there are regions that a charged particle cannot reach, whose size depends on Earth's magnetic field characteristics and the particle properties. These regions' boundary shrinkage or expansion in response to changes in the Earth's field may also serve as an indication of changes in trapped particles trajectories.

In the present work we analyze the consequences of the secular decrease of the axial dipole component of the geomagnetic field over aspects of trapped energetic particles in the Van Allen inner radiation belt that have not been analyzed so far: the mirror point altitude and the inner limit of the shielded region in Störmer theory. For this purpose, we take advantage of the theoretical analysis made by Heckman and Lindstrom (1972) and Schulz and Paulikas (1972) together with the previously derived scaling relations. The geomagnetic field secular variation considered is described in Sect. 2, followed by the theory and assumptions in Sect. 3. Results are presented in Sect. 4 and discussed in Sect. 5.

2 Geomagnetic field secular variation

The motion of a charged particle, even in a purely dipolar magnetic field, is complex and cannot be solved analytically. However, there are some key aspects that can be analyzed using fully analytical expressions under this simplified field. In order to be able to do this, we consider a centered dipolar geomagnetic field, aligned with the Earth's rotation axis, i.e. an axial dipole field.

Indeed, the current geomagnetic field is dominantly dipolar. At present, the dipolar component accounts for ∼93% of the mean square total field at the Earth's surface, and the axial dipole for ∼90%. These contributions increase further above the surface, reaching for example, at three R_E distance from Earth's center, to ∼99% and ∼97% respectively. In fact, the dipolar geometry has dominated the geomagnetic field through the historical era (e.g. Jackson et al. 2000). In addition, indirect magnetic measurements suggest that the field was dipole dominated during the Holocene (Gubbins et al. 2006; Poletti et al. 2018) and during much of the geological past as well (Siscoe 1976; Panovska et al. 2019; Biggin et al. 2020), though archeomagnetic and paleomagnetic field models are far less certain than the historical models which are based on direct measurements. While the axial dipole dominance may decrease and even collapse during geomagnetic reversal transitions, the field recovers to spend most of its time in an axial dipole dominated configuration (Siscoe 1976; Biggin et al. 2020). Considering thus the secular variation of a pure axial dipolar field, which means taking into account only time changes in the axial dipolar moment, M_z, is a sensible approximation, especially far from Earth's core.

For this purpose, we considered M_z estimated from ${g_1}^0$ Gauss coefficient in IGRF-13 (Alken et al. 2021), that is $M_z = {g_1}^0 {R_E}^3$. Its time evolution is shown in Fig. 1. The full centered dipole moment intensity M is also shown for comparison where $M = [({g_1}^0)^2 + ({g_1}^1)^2 + ({h_1}^1)^2]^{1/2} {R_E}^3$. Both present almost the same decreasing rate of ∼0.06% per year. The small mean difference between M and M_z throughout the period 1900-2020, which does not exceed 2%, reflects the relatively small dipole tilt of ∼10-11.5° with respect to the rotation rate (Amit and Olson 2008).

3 Theory and method

3.1 General effects of axial dipolar moment variation on trapped particles in radiation belts

The theory used to assess the consequences of geomagnetic field secular variation over the mirror point height and the Störmer forbidden region boundary is mainly described in Heckman and Lindstrom (1972) and Schulz and Paulikas (1972). We start from their theoretical analysis of a particle's motion in an ideal axial dipolar field, with moment M_z, considering the three adiabatic invariants: μ associated with the motion around field lines (gyromotion) and expressing

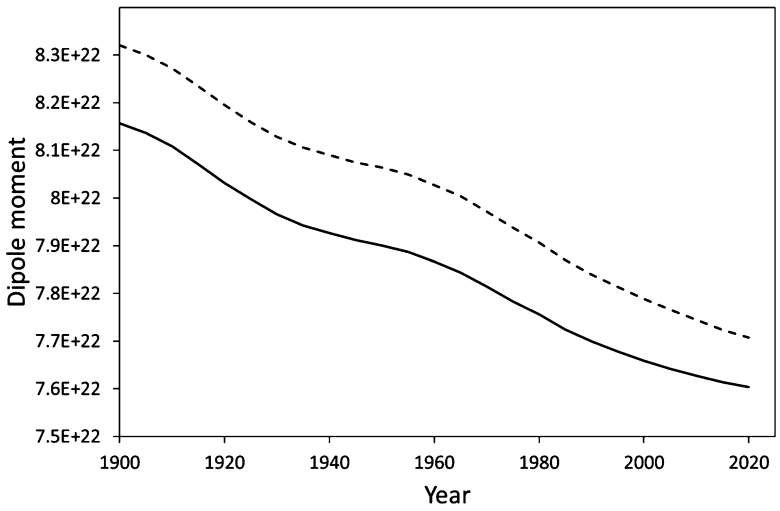

Fig. 1 Time evolution of the dipolar moment of Earth's magnetic field in Am^2 obtained from degree 1 Gauss coefficients in IGRF-13 for an axial dipole (M_z; solid line) and a full centered dipole (M; dashed line)

the conserved magnetic flux enclosed by the particle's gyromotion, J associated with the bouncing motion along the magnetic field between mirror points and implying the conserved total length of the particle trajectory along this line, and Φ associated with the azimuthal drift around the Earth and representing the conserved magnetic flux encompassed by the guiding drift shell. The conservation of the third invariant for an axial dipolar field is given by

$$\Phi = \frac{2\pi M_z}{L} \tag{6}$$

that is, the ratio L/M_z is also conserved. In terms of the rates of temporal change this implies that

$$\frac{1}{L}\frac{dL}{dt} = \frac{1}{M_z}\frac{dM_z}{dt} \tag{7}$$

Another way of deducing the L decrease induced by a weakening field is through Faraday's law. A time varying magnetic field $\boldsymbol{B}$ will induce an electric field $\boldsymbol{E}_{\text{ind}}$ given by

$$\oint \boldsymbol{E}_{\text{ind}} \cdot d\boldsymbol{l} = \iint \frac{\partial \boldsymbol{B}}{\partial t} \cdot d\boldsymbol{S} = \oint \frac{\partial \boldsymbol{A}}{\partial t} \cdot d\boldsymbol{l} \tag{8}$$

where $\boldsymbol{A}$ is the magnetic vector potential, which for an axial dipolar field in polar or cylindrical coordinates has only an azimuthal component, A_φ, given by

$$A_\varphi = \frac{\mu_o}{4\pi}\frac{M_z}{r^2}\cos\lambda \tag{9}$$

where μ_o is the vacuum permeability, r is the radial distance and λ the latitude angle. Equation (8) results then

$$\boldsymbol{E}_{\text{ind}} = -\frac{\mu_o}{4\pi}\frac{\cos\lambda}{r^2}\frac{dM_z}{dt}\hat{\varphi} \tag{10}$$

This induced field has an azimuthal direction and produces a drift which results from the cross product of $\boldsymbol{E}_{\text{ind}}$ and $\boldsymbol{B}$. For a decreasing M_z the drift direction will be inward for positive and negative charges, producing a shell contraction and particles' energization, while it will be outward for an M_z increase producing a shell expansion (see Chap. 3 in Roederer and Zhang 2014). Given that it is not easy to estimate the shell shrinking following this reasoning, an alternative approach relies on the third invariant, given by Equation (6) which allows an easy estimation of the drift shell contraction for a decreasing M_z (Heckman and Lindstrom 1972; Schulz and Paulikas 1972).

The variation in M_z implies also changes in the magnetic field intensity B along the particle's trajectory. For an axial dipolar field $B\alpha M_z/L^3$ and accounting for (7) results

$$\frac{1}{B}\frac{dB}{dt} = -\frac{2}{M_z}\frac{dM_z}{dt} \tag{11}$$

From the conservation of the first and second adiabatic invariants, the invariance of α and of λ_m are also deduced. In addition, the following relation holds for the particle's moment, p,

$$\frac{1}{p}\frac{dp}{dt} = -\frac{1}{M_z}\frac{dM_z}{dt} \tag{12}$$

In terms of the nonrelativistic kinetic energy, E, this condition can be written as

$$\frac{1}{E}\frac{dE}{dt} = -\frac{2}{M_z}\frac{dM_z}{dt} \tag{13}$$

3.2 Assumptions

One of the key aspects of a trapped particle's motion in Earth's magnetic field is its bounce motion between mirror points along a field line, and in particular the mirror point height, r_m (measured from the Earth's center) or $h_m = r_m - R_E$ (measured from the Earth's surface). In order to

obtain an analytical expression for the mirror point altitude in terms of M_z (Sect. 3.3) and its time variation considering the theory described in Sect. 3.1, and in order to deduce the changes in the Störmer forbidden region boundary through the time derivative of this boundary equation (Sect. 3.4), we apply the following assumptions:

(1) Conservation of particle's magnetic moment, μ (that is the first adiabatic invariant), in its gyro-motion around the magnetic field line, which is given by

$$\mu = \frac{m v_\perp^2}{2B} \tag{14}$$

where $v_\perp$ is the particle's velocity component perpendicular to the magnetic field line, m is its mass and B is the magnetic field intensity at the point under consideration. This means that the magnetic field variation in space is very small within a gyro-radius, and that the timescale of variation is much longer than the gyro-period.

(2) Conservation of the kinetic energy. This implies that

$$v_\parallel^2 + v_\perp^2 = \text{constant} \tag{15}$$

where $v_{||}$ is the particle's velocity component parallel to the magnetic field line.

(3) Drift motion around the Earth is negligible with respect to bouncing motion along the field line, which also guarantees the validity of the adiabatic invariants.

3.3 Mirror point altitude

Considering the field equation for an axial dipole, the radial distance of the mirror point, r_m, is

$$r_m = L R_\mathrm{E} (\cos\lambda_m)^2 \tag{16}$$

where λ_m is the latitude of the mirror point. This latitude position can be estimated from the pitch angle when the particle is at the magnetic equator, α_{eq}, through (Soni et al. 2020)

$$\left(\sin\alpha_{eq}\right)^2 = \frac{(\cos\lambda_m)^6}{\sqrt{1+3(\sin\lambda_m)^2}} \tag{17}$$

From Eqs. (16) and (17) it can be deduced that r_m (or h_m) does not depend neither on the particle's energy nor on the magnetic field intensity, just on the pitch angle and the line upon which it is bouncing given by L.

The temporal variation of r_m as a consequence of the geomagnetic field secular variation will be determined by that of L which can be estimated from Eq. (7). Differentiating Eq. (16) by time and substituting Eq. (7) gives

$$\frac{dr_m}{dt} = R_\mathrm{E} (\cos\lambda_m)^2 \frac{L}{M_z}\frac{dM_z}{dt} \tag{18}$$

Assuming that the height, h, at which trapped energetic particles are lost due to their interaction with a dense enough atmosphere is $h \leq 500$ km, then all charged particles trapped in shells where r_m is such as to lower h_m to 500 km or less will be lost or absorbed by the atmosphere. Considering r_m at 1900 as an initial value, its time evolution is forward iterated using Eqs. (16) and (18) in steps of 5 years (that is the time resolution of IGRF g_1^0 coefficient to estimate M_z). Because the re-organization time of the geomagnetic axial dipole is on the order of ~1000 years (Amit et al. 2018), the 5-year time step is clearly small enough to guarantee proper numerical resolution.

3.4 Störmer forbidden region boundary

Störmer (1955) showed that there are regions that a charged particle cannot access. By analyzing the Hamiltonian of the motion of a charged particle in an axial dipolar magnetic field (that is with azimuthal symmetry), he reduced the problem to the motion in a potential field where the potential function provides qualitative information about the resulting motion (Stern 1974). Although there are two constants of motion, the energy and the azimuthal component of the canonical momentum, they are not enough to provide an analytical solution for the motion. In a breakthrough contribution, Störmer (1955) noticed that the constancy of azimuthal canonical moment reduced the Hamiltonian to that of a motion in a two-dimensional potential. By qualitative arguments based on this potential, he deduced the existence of trapped orbits in the dipole field and of forbidden regions whose boundaries can be deduced analytically from the Hamiltonian or Lagrangian equation, as is the case of Eq. (19).

The size of these regions depends on Earth's magnetic field characteristics, that is M_z for the field here considered, and some particle properties, which are its charge, q, mass, m, and energy, E. The boundary of this region is defined by the equation for its distance from the Earth's center, r, in terms of the latitude angle, λ (Störmer 1955; Shepherd and Kress 2007)

$$r = \sqrt{\frac{\mu_o}{4\pi}\frac{M_z q}{\sqrt{2Em}}}\frac{(\cos\lambda)^2}{1+\sqrt{1+(\cos\lambda)^3}} \tag{19}$$

The root factor corresponds to the Störmer length, C_st.

A decrease in M_z clearly induces an approach of this boundary towards the Earth's surface. Considering also that E increases with M_z decrease according to Eq. (13), it would enhance the boundary approach towards the Earth. Taking the temporal derivative of r, and considering the temporal variations of M_z and E, the following equation is obtained

$$\frac{dr}{dt} = \frac{1}{2}r\frac{1}{M_z}\frac{dM_z}{dt} - \frac{1}{4}r\frac{1}{E}\frac{dE}{dt} = r\frac{1}{M_z}\frac{dM_z}{dt} \tag{20}$$

Equation (19) cannot be readily solved for the time evolution of r because E is unknown. However, Eq. (20) is independent of E hence can be used to forward iterate r in time. Finally, we normalize the solution by the initial value of r at 1900 to obtain a non-dimensional Störmer forbidden region boundary which is independent of any choice of an initial E.

4 Results

4.1 Mirror point altitude

Figure 2 shows the time variation of λ_m and h_m, for three different initial (i.e. at 1900) altitudes corresponding to three different initial values of L: 1.16 (∼1000 km above Earth's surface), 1.5, and 2. The 500 km mirror point height level is shown as a dashed black line, to indicate that at lower heights charged particles are lost in the atmosphere. It can be clearly seen that as M_z decreases with time h_m approaches the atmosphere, and that this approach is slower for higher λ_m. It is fastest for particles bouncing close to the equator, that is at low λ_m, but the trapped particles perform their trajectories in this case, for a given L value, much higher. This can be deduced from Eq. (6), since for a fixed L value, a lower λ_m results in a $\cos(\lambda_m)$ factor closer to 1 and thus a higher r_m.

For larger L values, the particle can mirror at higher latitudes. This is logical considering that the Earth has a finite volume, and for a dipolar field assuming there is no atmosphere surrounding the Earth, the maximum attainable λ_m would correspond to the invariant latitude, Λ, of a given L at the Earth surface, that is

$$\cos\Lambda = \sqrt{\frac{1}{L}} \tag{21}$$

In other words the maximum attainable λ_m is the latitude where a magnetic field line touches the Earth. For $L = 1.16$, 1.5 and 2, $\Lambda = 22.4, 35.3$ and 45 degrees respectively, which corresponds to the maximum λ_m for 1900 in each panel of Fig. 2. As M_z decreases, L decreases also and consequently Λ, or the maximum attainable λ_m (for a dipolar field assuming that a particle can reach the Earth's surface as the closer mirror distance) is also observed to decrease. That is the downward slope with time noticed for each height level in Fig. 2.

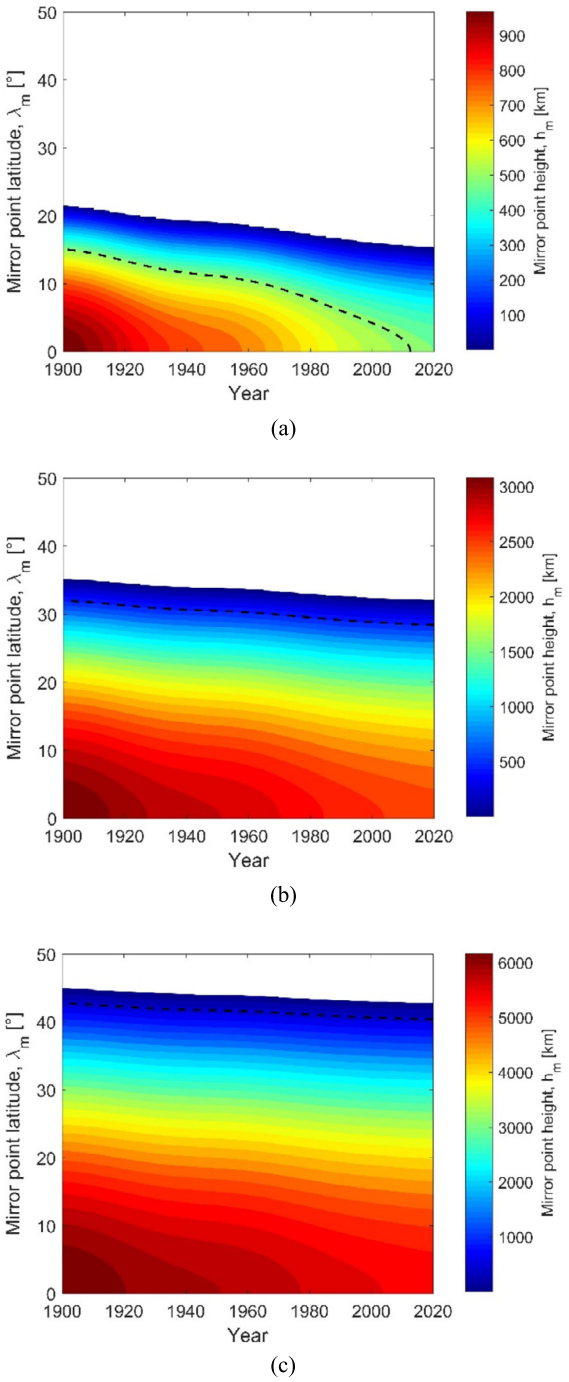

Fig. 2 Variation of the mirror point height, h_m [km], corresponding to a given mirror point latitude, λ_m [°], with the Earth's axial dipole moment variation during 1900-2020, for initial $L(t = 1900) = 1.16$ (**a**), 1.5 (**b**) and 2 (**c**). The axial dipole moment is estimated from the time-dependent g_1^0 Gauss coefficient in IGRF-13. Dashed black lines indicate 500 km height

4.2 Inner limit of the shielded region in Störmer theory

Figure 3 shows the boundary of the forbidden region, in a meridional plane, considering M_z in 1900 (solid), for a proton of 2 GeV energy as an example. Its numerically iterated displacement to lower latitudes in 2020 taking into account M_z and E temporal variations, where dr/dt is estimated from Eq. (20), is also shown (dashed). Taking into account the axial symmetry and also the symmetry with respect to

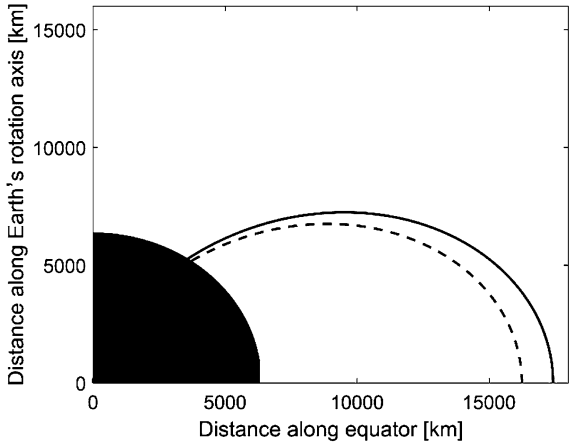

Fig. 3 Boundaries of Störmer forbidden region estimated with Eq. (19) considering M_z in 1900 (solid line) and with Eq. (20) to estimate the boundary in 2020 (dashed line). (Note: origin is the Earth's center; black surface is the Earth)

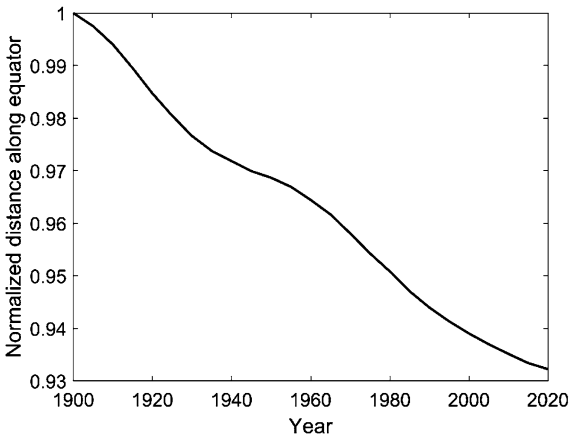

Fig. 4 Time dependence of the distance of the Störmer forbidden region from the Earth's center at the equatorial plane, normalized to its initial value in 1900, $r(1900)$, estimated from Eq. (19) and its temporal variation forward iterated from Eq. (20)

the equatorial plane, this figure illustrates a quadrant of the meridian plane where the abscissa corresponds to $r\cos(\lambda)$ and the ordinate to $r\sin(\lambda)$.

Figure 4 presents the time variation of the distance of the Störmer forbidden region from the Earth's center at the equator, which is $(\sqrt{2}-1)C_{\rm st}$.

Even though $C_{\rm st}$, used here as a proxy for the trapped particles drift shell contraction, is too distant for some regular particles trapped in the Earth's radiation belts (Lemaire 2003) as compared to their theoretical drift shells, it clearly shows how the shield provided by the geomagnetic field approaches the Earth's surface as M_z decreases. In the 120 years studied period, the distance of this shield to Earth's surface decreased by ~7% (Fig. 4), at the same rate as the decrease of the geomagnetic axial dipole (Fig. 1). In addition, the well-known non-linear undulations with typical periodicity of ~60 years observed in the geomagnetic axial dipole secular variation (Olson and Amit 2006; Buffett 2014; Buffett et al. 2016; Finlay et al. 2016; Huguet et al. 2018) correlate well with the undulations in the inner limit of the shielded region (Fig. 4).

5 Discussion

The motion of charged particles trapped in radiation belts by the Earth's magnetic field is complicated even for the axial dipolar field approximation. It can be simplified for a slowly varying purely axial dipole field by decomposing the total motion into three components: gyration around a guiding field line, bounce along this line between mirror points, and drift in the azimuthal direction around the Earth. For a static dipolar magnetic field, and in the absence of any loss mechanism, these particles should remain stably trapped indefinitely following their trajectories in the magnetosphere. The time variation of the Earth's field is expected to cause changes in the particle's trajectory characteristics not only due to the dependence on the field, but also due to the force related to the induced electric field associated with the time-dependent magnetic field (Roederer and Zhang 2014). This can be easily taken into account if the field time variation is much slower than the corresponding timescale of each type of motion, as is the case for the secular variation here considered. This can be done by considering the third adiabatic invariant which leads to Eq. (2). In the axial dipolar field assumed in the present work, a decrease of the dipole moment causes the guiding drift shells to contract, and this change in drift shell is accompanied by a change in particle energy given by Eq. (13).

Considering the actual secular change in M_z associated to the axial dipolar field, we calculated for the first time the temporal evolution of the mirror point height and the boundary of the Störmer forbidden region. Both quantities decrease, as qualitatively expected from a drift shell contraction, at the same percentage rate as M_z does. Their absolute changes, however, depend not only on M_z but on L and $\alpha_{\rm eq}$ (or λ_m) in the case of the mirror point height, and on energy and particle type as well in the case of the boundary of the Störmer forbidden region.

If we compare the variations in h_m and the boundary of the Störmer forbidden region to the magnetopause approach which can be estimated from the scaling relation in Equation (1), a much slower approach is obtained for the latter. In fact, $R_{\rm mp}$ rate of change with M_z, considering steady solar wind conditions, would be

$$\frac{1}{R_{mp}}\frac{dR_{mp}}{dt} = \frac{1}{3}\frac{1}{M_z}\frac{dM_z}{dt} \tag{22}$$

that is one third of h_m and C_{st} rate of change. This means that, if we were able to extrapolate our hypothesis without

limits, there would be a period of time with a magnetosphere cavity surrounding the Earth but not acting as a shield.

An interesting aspect to consider in future works would be the comparison between h_m decrease induced by the secular geomagnetic field dipolar component weakening, and the shrinking of the upper atmosphere due to the cooling induced by greenhouse gases increasing concentration during the last decades (Lastovicka 2021). There will be particles whose mirror points altitudes' lowering would result in their absorption and loss, unless it is smaller than the atmosphere contraction due to its long-term cooling.

Acknowledgements Argentina's Consejo Interuniversitario Nacional provided financial support to A.R. Gutierrez Falcon through the research fellowship Beca-EVC-CIN. A.G. Elias and B.S. Zossi also acknowledge PIUNT E642 and PIP 2957. IGRF is freely available at https://www.ngdc.noaa.gov/IAGA/vmod/igrf.html.

Author Contribution All authors contributed to the study and design of this work. The first draft of the manuscript was written by A.R. Gutierrez Falcon and A.G. Elias and all authors commented on previous versions of the manuscript. All authors read and approved the final manuscript.

Funding A.R. Gutierrez Falcon has received funding from Argentina's Consejo Interuniversitario Nacional through the research fellowship Beca-EVC-CIN. A.G. Elias and B.S. Zossi have received research support from CONICET, grant number: PIP 11220200102957CO.

Data Availability Data sharing not applicable to this article as no datasets were generated or analysed during the current study.

Declarations

Ethical statement All authors comply with ethical standards.

Conflict of Interest The authors declare they have no financial interests.

References

Alken, P., Thebault, E., Beggan, C.D., et al.: International Geomagnetic Reference Field: the thirteenth generation. Earth Planets Space **73**, 49 (2021). https://doi.org/10.1186/s40623-020-01288-x

Amit, H., Olson, P.: Geomagnetic dipole tilt changes induced by core flow. Phys. Earth Planet. Inter. **166**, 226–238 (2008). https://doi.org/10.1016/j.pepi.2008.01.007

Amit, H., Coutelier, M., Christensen, U.R.: On equatorially symmetric and antisymmetric geomagnetic secular variation timescales. Phys. Earth Planet. Inter. **276**, 190–201 (2018). https://doi.org/10.1016/j.pepi.2017.04.009

Aubert, J.: Geomagnetic forecasts driven by thermal wind dynamics in Earth's core. Geophys. J. Int. **203**, 1738–1751 (2015). https://doi.org/10.1093/gji/ggv394

Aubert, J., Finlay, C.C., Fournier, A.: Bottom-up control of geomagnetic secular variation by the Earth's inner core. Nature **502**, 219–223 (2013). https://doi.org/10.1038/nature12574

Biggin, A.J., Bono, R.K., Meduri, D.G., et al.: Quantitative estimates of average geomagnetic axial dipole dominance in deep geological time. Nat. Commun. **11**, 6100 (2020). https://doi.org/10.1038/s41467-020-19794-7

Bloxham, J., Gubbins, D., Jackson, A.: Geomagnetic secular variation. Philos. Trans. R. Soc. Lond. Ser. A, Math. Phys. Sci. **329**, 415–502 (1989). https://doi.org/10.1098/rsta.1989.0087

Boscher, D., Sicard-Piet, A., Lazaro, D., Cayton, T., Rolland, G.: A new proton model for low altitude high energy specification. IEEE Trans. Nucl. Sci. **61**, 3401–3407 (2014). https://doi.org/10.1109/TNS.2014.2365214

Bourdarie, S., Fournier, A., Sicard, A., Hulot, G., Aubert, J., Standarovski, D., Ecoffet, R.: Impact of the Earth's magnetic field secular drift on the low altitude proton radiation belt from years 1900 to 2050. IEEE Trans. Nucl. Sci. **66**, 1746–1752 (2019). https://doi.org/10.1109/TNS.2019.2897378

Buffett, B.A.: Geomagnetic fluctuations reveal stable stratification at the top of the earth's core. Nature **507**, 484–487 (2014). https://doi.org/10.1038/nature13122

Buffett, B.A., Knezek, N., Holme, R.: Evidence for MAC waves at the top of Earth's core and implications for variations in length of day. Geophys. J. Int. **204**, 1789–1800 (2016). https://doi.org/10.1093/gji/ggv552

Cnossen, I., Richmond, A.D., Wiltberger, M.: The dependence of the coupled magnetosphere-ionosphere-thermosphere system on the Earth's magnetic dipole moment. J. Geophys. Res. **117**, A05302 (2012). https://doi.org/10.1029/2012JA017555

Farley, T.A., Kivelson, M.G., Wait, M.: Effects of the Secular Magnetic Variation on the Distribution Function of Inner-Zone Protons. J. Geophys. Res. **77**, 6087 (1972). https://doi.org/10.1029/JA077i031p06087

Fei, Y., Chan, A.A., Elkington, S.R., Wiltberger, M.J.: Radial diffusion and MHD particle simulations of relativistic electron transport by ULF waves in the September 1998 storm. J. Geophys. Res. **111**, A12209 (2006). https://doi.org/10.1029/2005JA011211

Feynman, J., Ruzmaikin, A.: The Centennial Gleissberg Cycle and its association with extended minima. J. Geophys. Res. **119**, 6027–6041 (2014). https://doi.org/10.1002/2013JA019478

Finlay, C.C.: Historical variation of the geomagnetic axial dipole. Phys. Earth Planet. Inter. **170**, 1–14 (2008). https://doi.org/10.1016/j.pepi.2008.06.029

Finlay, C.C., Aubert, J., Gillet, N.: Gyre-driven decay of the Earth's magnetic dipole. Nat. Commun. **7**, 10422 (2016). https://doi.org/10.1038/ncomms10422

Glassmeier, K.H., Vogt, J., Stadelmann, A., Buchert, S.: Concerning long-term geomagnetic variations and space climatology. Ann. Geophys. **22**, 3669–3677 (2004). https://doi.org/10.5194/angeo-22-3669-2004

Gubbins, D., Jones, A.L., Finlay, C.C.: Fall in Earth's Magnetic Field Is Erratic. Science **312**, 900–902 (2006). https://doi.org/10.1126/science.1124855

Heckman, H.H., Lindstrom, P.J.: Response of trapped particles to a collapsing dipole moment. J. Geophys. Res. **77**, 740–743 (1972). https://doi.org/10.1029/JA077i004p00740

Heirtzler, J.R.: The Future of the South Atlantic Anomaly and implications for radiation damage in space. J. Atmos. Sol.-Terr. Phys. **64**, 1701–1708 (2002). https://doi.org/10.1016/S1364-6826(02)00120-7

Huguet, L., Amit, H., Alboussiere, T.: Geomagnetic Dipole Changes and Upwelling/Downwelling at the Top of the Earth's Core. Front. Earth Sci. **6**, 170 (2018). https://doi.org/10.3389/feart.2018.00170

Jackson, A., Jonkers, A.R.T., Walker, M.R.: Four centuries of geomagnetic secular variation from historical records. Philos. Trans. R. Soc. A **358**, 957–990 (2000). https://doi.org/10.1098/rsta.2000.0569

Lastovicka, J.: Long-Term Trends in the Upper Atmosphere. In: Wang, W., Zhang, Y., Paxton, L.J. (eds.) Upper Atmosphere Dynamics and Energetics, pp. 325–344. Am. Geophys. Union, Washington (2021)

Lemaire, J.F.: The effect of a southward interplanetary magnetic field on Störmer's allowed regions. Adv. Space Res. **31**, 1131–1153 (2003). https://doi.org/10.1016/S0273-1177(03)00099-1

Lindstrom, P.J., Heckman, H.H.: B-L Space and Geomagnetic Field Models. J. Geophys. Res. **73**, 3441–3447 (1968). https://doi.org/10.1029/JA073i011p03441

McIlwain, C.E.: Coordinates for mapping the distribution of magnetically trapped particles. J. Geophys. Res. **66**, 3681–3691 (1961). https://doi.org/10.1029/JZ066i011p03681

Olson, P., Amit, H.: Changes in earth's dipole. Naturwissenschaften **93**, 519–542 (2006). https://doi.org/10.1007/s00114-006-0138-6

Panovska, S., Korte, M., Constable, C.G.: One hundred thousand years of geomagnetic field evolution. Rev. Geophys. **57**, 1289–1337 (2019). https://doi.org/10.1029/2019RG000656

Poletti, W., Biggin, A.J., Trindade, R.I.F., Hartmann, G.A., Terra-Nova, F.: Continuous millennial decrease of the Earth's magnetic axial dipole. Phys. Earth Planet. Inter. **274**, 72–86 (2018). https://doi.org/10.1016/j.pepi.2017.11.005

Pu, Z.Y., Xie, L., Fang, X.H., Jiao, W.X., Fu, S.Y., Zong, Q.G.: Drift Shell Tracing and Secular Variation of Inner Radiation Environment in the SAA Region. COSPAR Colloq. Ser. **14**, 353–358 (2002). https://doi.org/10.1016/S0964-2749(02)80181-0

Roederer, J.G., Zhang, H.: Dynamics of Magnetically Trapped Particles, Foundations of the Physics of Radiation Belts and Space Plasmas, 2nd edn. Springer, Berlin (2014)

Saito, T., Sakurai, T., Yumoto, K.: The Earth's palaeomagnetosphere as the third type of planetary magnetosphere. Planet. Space Sci. **26**, 413–422 (1978). https://doi.org/10.1016/0032-0633(78)90063-6

Sanchez, S., Wicht, J., Bärenzung, J.: Predictions of the geomagnetic secular variation based on the ensemble sequential assimilation of geomagnetic field models by dynamo simulations. Earth Planets Space **72**, 157 (2020). https://doi.org/10.1186/s40623-020-01279-y

Schulz, M.: Paleomagnetospheric radial diffusion. Geophys. Res. Lett. **2**, 173–175 (1975). https://doi.org/10.1029/GL002i005p00173

Schulz, M., Paulikas, G.A.: Secular Magnetic Variation and the Inner Proton Belt. J. Geophys. Res. **77**, 744–747 (1972). https://doi.org/10.1029/JA077i004p00744

Shepherd, S.G., Kress, B.T.: Störmer theory applied to magnetic spacecraft shielding. Space Weather **5**, S04001 (2007). https://doi.org/10.1029/2006SW000273

Siscoe, G.L.: Two magnetic tail models for 'Uranus'. Planet. Space Sci. **19**, 483–490 (1971). https://doi.org/10.1016/0032-0633(71)90164-4

Siscoe, G.L.: Long-term aspects of magnetospheric variability. In: Physics of Solar Planetary Environments: Proceedings of the International Symposium on Solar-Terrestrial Physics, June 7–18, 1976, Boulder, Colorado, vol. II, pp. 973–1004 (1976)

Siscoe, G.L., Chen, C.K.: The paleomagnetosphere. J. Geophys. Res. **80**, 4675–4680 (1975). https://doi.org/10.1029/JA080i034p04675

Soni, P.K., Kakad, B., Kakad, A.: L-shell and energy dependence of magnetic mirror point of charged particles trapped in Earth's magnetosphere. Earth Planets Space **72**, 129 (2020). https://doi.org/10.1186/s40623-020-01264-5

Stadelmann, A., Vogt, J., Glassmeier, K.H., Kallenrode, M.B., Voigt, G.H.: Cosmic ray and solar energetic particle flux in paleomagnetospheres. Earth Planets Space **62**, 333–345 (2010). https://doi.org/10.5047/eps.2009.10.002

Stern, D.P.: Charged particle motions in a magnetic field that reduce to motions in a potential. Am. J. Phys. **43**, 689–694 (1974). https://doi.org/10.1119/1.9714

Störmer, C.: The Polar Aurora. Oxford University Press, New York (1955)

Tarduno, J.A.: Subterranean clues to the future of our planetary magnetic shield. Proc. Natl. Acad. Sci. USA **115**, 13154–13156 (2018). https://doi.org/10.1073/pnas.1819025116

Terra-Nova, F., Amit, H., Hartmann, G.A., Trindade, R.I.F., Pinheiro, K.J.: Relating the South Atlantic Anomaly and geomagnetic flux patches. Phys. Earth Planet. Inter. **266**, 39–53 (2017). https://doi.org/10.1016/j.pepi.2017.03.002

Tsareva, O.O., Zelenyi, L.M., Malova, K.V., Popov, V.Y.: Radiation Belts during a Magnetic Field Reversal. Cosm. Res. **58**, 227–233 (2020). https://doi.org/10.1134/S0010952520040103

Vogt, J., Glassmeier, K.H.: On the location of trapped particle populations in quadrupole magnetospheres. J. Geophys. Res. **105**, 13063–13071 (2000). https://doi.org/10.1029/2000JA900006

Vogt, J., Glassmeier, K.H.: Modelling the paleomagnetosphere: Strategy and first results. Adv. Space Res. **28**, 863–868 (2001). https://doi.org/10.1016/S0273-1177(01)00504-X

Vogt, J., Zieger, B., Glassmeier, K.H., Stadelmann, A., Kallenrode, M.B., Sinnhuber, M., Winkler, H.: Energetic particles in the paleomagnetosphere: Reduced dipole configurations and quadrupolar contributions. J. Geophys. Res. **112**, A06216 (2007). https://doi.org/10.1029/2006JA012224

Zieger, B., Vogt, J., Glassmeier, K.H.: Scaling relations in the paleomagnetosphere derived from MHD simulations. J. Geophys. Res. **111**, A06203 (2006). https://doi.org/10.1029/2005JA011531